Electric and Magnetic Properties of a Neutral Radical, 2-Cyano-10-methyl-5-phenazinyl

Kunio AWAGA, Tadashi SUGANO, and Minoru KINOSHITA*
The Institute for Solid State Physics, The University of Tokyo, Roppongi, Minato-ku, Tokyo 106
(Received March 8, 1985)

The temperature dependence of electric conductivity, static magnetic susceptibility and ESR absorption, and electronic absorption spectra at room temperature have been measured on an organic neutral radical, 2-cyano-10-methyl-5-phenazinyl (NMPN). NMPN is found to be more conductive than the neutral radicals studied previously. The room temperature conductivity of powder NMPN is of the order of $10^{-7}\,\Omega^{-1}\,cm^{-1}$ and the activation energy is 0.36 eV. The absorption spectra and the magnetic susceptibility measurements indicate that the NMPN molecules form pairing array with considerably large interpair interaction in the solid state. The absence of the triplet fine structure in the ESR spectrum also suggests the existence of the interpair interaction. From these, the magnetic behavior of NMPN is interpreted in terms of the alternating antiferromagnetic Heisenberg model with temperature dependent alternation.

The electrical conduction of organic solids has been a matter of concern for long time and the efforts to find out highly conducting materials among the organic solids composed of one kind of molecules have been continued. Especially, the conduction of aromatic hydrocarbons represented by anthracene has been studied in detail.[1] However, it is known that most of them show the conductivity of less than $10^{-10}\,\Omega^{-1}\,cm^{-1}$ at room temperature and the activation energy of several eV (1 eV/molecule≒96.48 kJ mol^{-1}). One of the reasons for poor conductivity is that in the ground state no carriers can exist because the component molecules take the closed shell structure.

In this regards, the electrical conduction of a neutral free radical, which has intrinsically one unpaired electron giving the expectancy of becoming a carrier, has been interested in. Table 1 (a)—(c) shows the electric conductivities of the neutral radicals studied previously.[2-4] Contrary to expectation, they exhibit poor conductivity in spite of the presence of unpaired electrons. The reason for this is considered to be as follows. These radicals are characterized commonly by having protective substituents to stabilize the unpaired electron.[5,6] The protective substituents must obstruct the interactions between the unpaired electrons and therefore the unpaired electrons would be localized on each site of radical molecules. Above consideration is supported by the fact that the magnetic behavior of these radicals follow the Curie-Weiss law with small Weiss constants, representing the localized character of spins. Taking it the other way round, it would be predicted that using a planar radical molecule leads to increase of the interactions and to improvement of the conductivity.

To confirm this prediction, we have chosen 2-cyano-10-methyl-5-phenazinyl(commonly called *N*-methylphenazyl-2-nitrile; abbreviated as NMPN hereafter) shown in Fig. 1 as an experimental sample, which has planar molecular structure and is stabilized mainly by the intramolecular delocalization of the unpaired electron. We have investigated the electric conductivity and further, to make the properties of NMPN clearer, the temperature dependence of the magnetic susceptibility and the electron spin resonance signals, and the absorption spectra at room temperature have been measured.

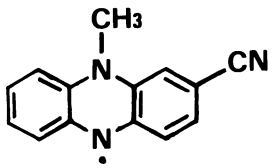

Fig. 1. The molecular structure of NMPN (2-cyano-10-methyl-5-phenazinyl).

In this paper, we characterize the electric and magnetic properties of NMPN using the results of the above experiments and discuss the electric conductivity of NMPN. From these, we suggest the way to improve the electric conductivity of a neutral free radical.

Experimental

NMPN was prepared by the method of McIlwain.[7] The crude NMPN obtained was purified by recrystallization from chloroform or a mixture of chloroform and diethyl ether, followed by washing with diethyl ether continuously (Found: C, 76.36; H, 4.36 N, 19.31%, Calcd for $C_{14}H_{10}N_3$: C, 76.35; H, 4.58; N, 19.08%). The purified samples were kept in a freezer, because they were gradually damaged when kept at room temperature.

The d.c. electric conductivity of compressed polycrystals was measured in a vacuum using the standard two-probe technique with the aid of Ag paint for electrodes.

The magnetic susceptibility was measured by using a Faraday balance on a powder sample of about 50 mg. The details of the apparatus have been described previously.[8] The measurement was taken over the con-

tinuous temperature range of 4—295 K.

A Cary model 14 spectrophotometer was used for measurements of the electronic absorption spectra of an ethanol solution and a solid sample suspended in liquid paraffin. The spectra were measured at room temperature in the range of 5000—30000 cm^{-1}.

Temperature dependence of X-band electron spin resonance (ESR) spectra from 10 to 300 K were performed on a JES-FE1X spectrometer with an Oxford Instruments ESR-900 variable temperature helium gas flow cryostat. In every measurement the modulation width was kept within 0.1 G (1 G=10^{-4}T) in order to prevent lineshape distortion due to over modulation.

Electrical and Magnetic Properties

Electric Conductivity. Figure 2 shows a plot of logarithm of the conductivity at absolute temperature T *vs.* $1/T$ for two specimens which were prepared in different butches. The discrepancy between the temperature dependence of the two specimens is within the experimental error. The conductivity at room temperature is of the order of $10^{-7}\ \Omega^{-1}\ cm^{-1}$. Below 350 K, the linear relation between logarithm of the conductivity and $1/T$ is established well. Above 350 K, the conductivity decreases abruptly. After keeping the samples above this temperature, the intensity of ESR signals vanishes almost completely. Therefore, the decrease of conductivity would be ascribed to the decomposition of radical molecules. In other words, the relatively high conductivity of NMPN observed below 350 K is attributable to the existence of an unpaired electron on each molecule.

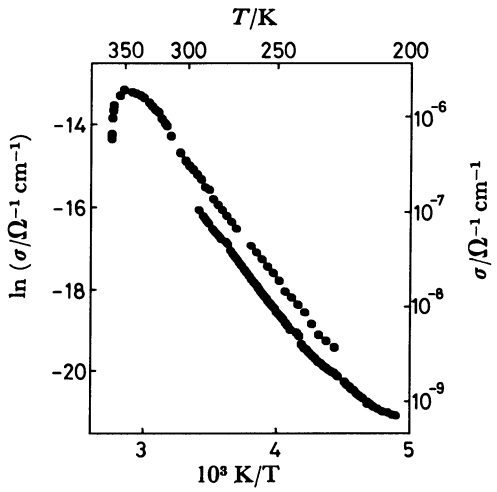

Fig. 2. Specific conductivity of NMPN for two specimens.

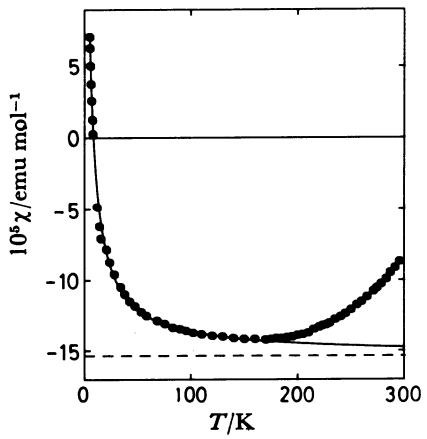

Fig. 3. Temperature dependence of total magnetic susceptibility of NMPN. The dashed line represents the diamagnetic susceptibility. The solid curve represents the paramagnetic one due to impurities.

The activation energy is computed from the change of conductivity as a function of temperature using the equation

$$\sigma = \sigma_0 \exp(-\Delta/k_B T), \quad (1)$$

where σ is the specific conductivity at T, σ_0 is a constant, k_B is the Boltzmann constant and Δ is the activation energy. The slope below 350 K corresponds to the activation energy of 0.36 eV. NMPN shows relatively high conductivity and low activation energy among the organic solids composed of one kind of molecules.

Table 1 shows the comparison of the electric conductivity of NMPN and that of the neutral free radicals investigated previously.[2-4] The latter radicals are stabilized by the protective substituents.[5,6] The conductivity of NMPN is higher than that of the other radicals by more than three orders of magnitude. The activation energy of NMPN is about a half as large as the others. The prediction made in the introductory section thus seems to be fulfilled.

Magnetic Susceptibility. Temperature dependence of the molar magnetic susceptibility of NMPN is shown in Fig. 3. In the high temperature region, the susceptibility decreases with decreasing temperature, and after passing a minimum it increases in the low temperature region. The diamagnetic contribution is evaluated by assuming that the susceptibility change in the low temperature region is dominated by the paramagnetic susceptibility due to impurities

Table 1. The comparison of the electric conductivity of the neutral radicals

		$\sigma_{25\,°C}$ / $\Omega^{-1}\ cm^{-1}$	Δ / eV	σ_0 / $\Omega^{-1}\ cm^{-1}$
(a)	DPPH (single crystal)	2×10^{-10}	0.75	10^3
(b)	Galvinoxyl	4×10^{-14}	0.72	0.07
(c)	Banfield and Kenyon's radical	3×10^{-15}	1.2	10^5
(d)	NMPN	3×10^{-7}	0.36	0.35

(a) in Ref. 4. (b), (c) in Ref. 3. (d) This work.

and/or defects which follows the Curie-Weiss law. The diamagnetic susceptibility thus obtained is -153×10^{-6} emu mol^{-1} [9] which is indicated by the dashed line in Fig. 3. The Curie-Weiss susceptibility with the Curie constant of 1.70×10^{-3} emu K mol^{-1}, corresponding to a spin concentration ($S=1/2$) of 0.45%, and with the Weiss constant of -2.66 K, is shown in Fig. 3 by the solid curve.

The intrinsic paramagnetic susceptibility χ_P, after correction for the diamagnetic and the Curie-Weiss parts have been made, is plotted as a function of temperature in Fig. 4. χ_P appears to increase exponentially from about 150 K. This shows existence of relatively strong antiferromagnetic interactions between the unpaired electrons and of the thermally accessible magnetic excitation state. By assuming that the antiferromagnetic interactions are limited only within a pair of spins, the temperature dependence of χ_P may be analyzed by the singlet-triplet model. The temperature dependence of the singlet-triplet susceptibility χ_{st} is given by

$$\chi_{st} = \frac{N_A g^2 \mu_B^2}{k_B T} \frac{1}{3+\exp(J/k_B T)}, \quad (2)$$

where N_A is the Avogadro constant, μ_B is the Bohr magneton, g is the g-value and J is the energy separation between the ground singlet state and the excited triplet state. The solid curves (a), (b), and (c) in Fig. 4 are theoretical curves of the singlet-triplet model for $J=0.11$, 0.12, and 0.13 eV, respectively. The temperature dependence of magnetic susceptibility of NMPN is found to fit only qualitatively to the singlet-triplet susceptibility, but does not fit quantitatively for any value of J. Such discrepancy between χ_P and χ_{st} has also been observed in various charge transfer complexes and the following explanations have been suggested.

1) The change in the intermolecular distance by thermal expansion.[10]

2) The phonon induced interaction between magnetic excitons.[11,12]

3) The existence of interpair interaction (*i.e.*, alternating antiferromagnetic chain).[13-17]

Further discussion will be given below by taking account of the results of the absorption spectra and the ESR measurements.

Electronic and ESR Spectra

Absorption Spectra. The temperature dependence of χ_P suggests that, within the first approximation, NMPN molecules exist in the solid as what is called "radical pair" formed by the charge transfer interaction.[18] In order to confirm the existence of the charge transfer interaction, absorption spectra were measured for an ethanol solution and a solid sample at room temperature. The comparison is shown in Fig. 5. The broad band at about 9000 cm^{-1} in the solid spectrum is much enhanced in comparison with that of the solution spectrum. Therefore, we could attribute this band to the charge transfer band. A weak absorption appears like shoulder at about 12000 cm^{-1}. Such a structure of a CT-band is also observed in Würster's blue perchlorate and alkali metal-TCNQ(7,7,8,8-tetracyano-*p*-quinodimethan) which are known as Mott insulators. Lyo has given two explanations for this phenomenon.

1) The effect of long-range Coulomb interaction.[19]

2) The charge transfer between pairs.[20]

On the basis of the experimental results of susceptibility and ESR, we will take the latter explanation in the later sections.

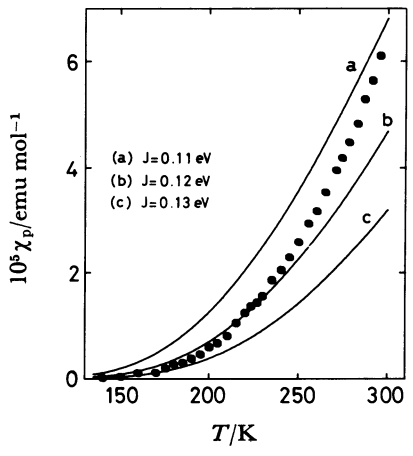

Fig. 4. Intrinsic paramagnetic susceptibility of NMPN. The solid curves are theoretical fits as explained in the text.

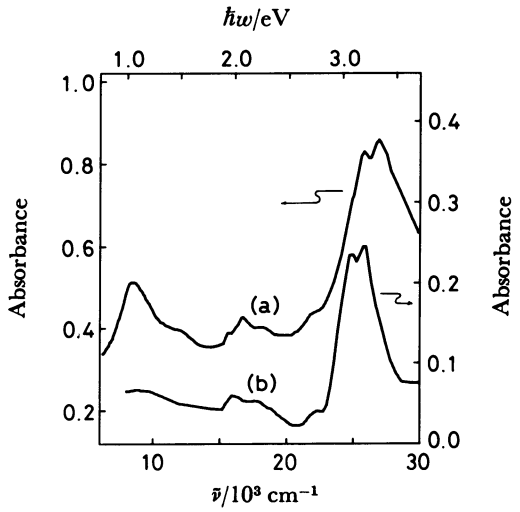

Fig. 5. Absorption spectra of NMPN at room temperature. (a): Powder sample suspended in liquid paraffin, (b): solution in ethanol.

The other absorption bands of solid NMPN correspond well to those of the solution spectrum except for blue shift of the strong absorption at about 27000 cm^{-1}. This blue shift would be explained by either the solvent effect or the coupling of CT and LE transitions.[21]

ESR Absorption. The ESR spectra observed on the powder sample at various temperatures are shown in Fig. 6, in which the three signals at lower temperatures are magnified by ten times. Asymmetric lineshape of the spectra in the high temperature region is due to *g*-value anisotropy. The *g*-value anisotropy disappears with broadening of the linewidth at low temperatures. Temperature dependence of the peak-to-peak linewidth ΔH_{pp} is shown in Fig. 7. Below 140 K, ΔH_{pp} increases abruptly with decrease of temperature and becomes constant at 80 K. Thus,

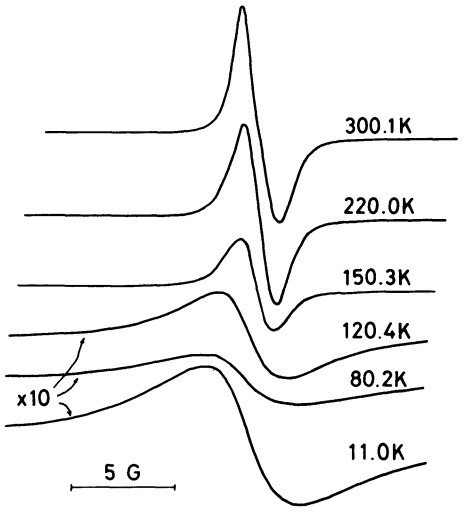

Fig. 6. ESR signals on powder sample at various temperatures.

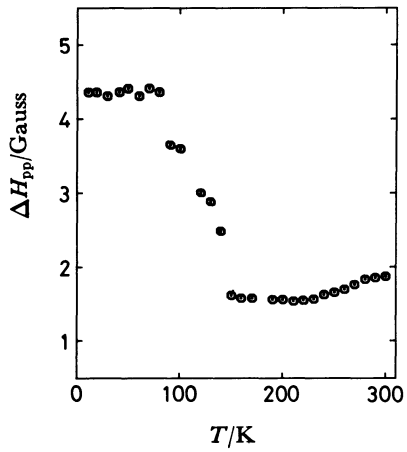

Fig. 7. Temperature dependence of ESR peak-to-peak linewidth, ΔH_{pp}.

the temperature dependence of ΔH_{pp} may be separated into the following three temperature regions.

In the high temperature region (T>140 K), the narrow linewidth signal, which increases in intensity with increasing temperature, is dominant. From the results of the static magnetic susceptibility, the observed ESR signals in this region should represent the spins excited thermally across the magnetic gap. The *g*-value anisotropy stands up with increasing temperature. Because the peak-to-peak linewidth in Fig. 7 is affected by the *g*-value anisotropy, we cannot place much significance on the variation of the linewidth in this temperature region. However, the true linewidth seems to depend little on temperature or to become narrower a little with increasing temperature.

In the low temperature region (T<90 K), the broad linewidth signal without *g*-value anisotropy, which increase in intensity with decreasing temperature, is dominant. These signals represent paramagnetic impurities observed in the susceptibility measurements. Their temperature independent linewidth suggests that the spins on the impurities are localized. The fact that the two kinds of signals observed in the high and low temperature regions have the same *g*-value suggests that the paramagnetic impurities are the localized spins on the monomer radicals, which have failed to form a pair structure during crystallization.

In the middle temperature region, the observed signals result from the two kinds of signals being piled up and therefore originate from the two kinds of spins discussed above. With decreasing temperature the linewidth increases abruptly and main contribution to the observed signals varies from the narrower signal to the broader one.

In order to examine whether or not the magnetic excited state is described by the triplet spin Hamiltonian:

$$\mathscr{H} = D\left(S_z^2 - \frac{2}{3}\right) + E(S_x^2 - S_y^2), \tag{3}$$

which represents the dipolar interaction in an isolated spin pair, we have tried to find out fine structure signals and $\Delta m = \pm 2$ transitions. The measurements were carefully done on the powder samples over the range of 90—300 K, but we could not find out both of them. This fact indicates that the spin system in NMPN is not simply described by an assembly of noninteracting spin pairs of Hamiltonian (3).

Analysis of Magnetic Susceptibility

The Model to be Used. From the experimental results described in the preceding sections, the

NMPN molecules are considered to be paired off, within the first approximation, by the charge transfer interaction in the solid state. Because this interaction needs the overlapping of the molecules and NMPN exhibits relatively high conductivity, it is reasonable to assume that the NMPN molecules form linearly stacking columns in the solid. The results of the ESR experiments suggest the existence of the interpair interaction. The discrepancy between the temperature dependence of the magnetic susceptibility observed and the singlet-triplet statistics would also be attributed to the interpair interactions as mentioned above. As a matter of course, this interpair interaction is weaker than the intrapair one, but seems to be so strong that the spin system in NMPN is not represented by the spin Hamiltonian (3). Therefore, the spins on the NMPN molecules are to be interpreted by a linear alternating antiferromagnetic Heisenberg model. As mentioned in a previous section, one of the explanations for the side band in the CT absorption region is also due to the coexistence of the intra- and interpair charge transfer interactions. The interpair charge transfer makes the two pair spins singlet just like the intrapair interaction.

Analysis. The Hamiltonian of the linear alternating antiferromagnetic Heisenberg model is given by

$$\mathscr{H} = \sum_{i=1}^{N/2} (J_1 \boldsymbol{S}_{2j}\boldsymbol{S}_{2j+1} + J_2 \boldsymbol{S}_{2j-1}\boldsymbol{S}_{2j}) = J_1 \sum_{i=1}^{N/2} (\boldsymbol{S}_{2j}\boldsymbol{S}_{2j+1} + \gamma \boldsymbol{S}_{2j-1}\boldsymbol{S}_{2j}) \quad (4)$$

where J_1 and J_2 are the alternating interactions along the chain (assumed as $J_1 > J_2 > 0$) and $\gamma = J_2/J_1$ is a parameter which conveniently measures the degree of alternation. When $\gamma=1$, the linear Heisenberg model is obtained, whereas when $\gamma=0$ the system breaks up into an assembly of noninteracting spin pairs.

Bulaevskii calculated the spectrum of triplet excitations of alternating chain of spins with the above Hamiltonian (4), by using the Hartree-Fock approximation.[13,14] His model has been used frequently in approximate theoretical treatments of a variety of phenomena. For example, it has been applied to charge-transfer salts,[22-24] to spin dynamics,[25] and to the uniform Heisenberg chain.[26]

On the other hand, Duffy and Barr[16] and Bonner *et al.*[17] have made exact calculations of the susceptibility on finite alternating antiferromagnetic Heisenberg spin-1/2 chains. The extrapolation of their results to $N \to \infty$ shows a good numerical agreement with the corresponding curves calculated from the model of Bulaevskii, especially at low temperatures.

In our case, the temperature region examined falls into the low temperature regions of these models. Therefore, we use the results of Bulaevskii for the analysis of the temperature dependence of the intrinsic paramagnetic susceptibility in Fig. 4. Bulaevskii has derived the following approximate equation at low temperatures ($0.033 < k_B T/J_1 < 0.25$)

$$\chi = \frac{N_A g^2 \mu_B^2 a(\gamma)}{k_B T} \exp\left(\frac{-J_1 \Delta(\gamma)}{k_B T}\right), \quad (5)$$

where $a(\gamma)$ and $\Delta(\gamma)$ are γ dependent parameters whose values are given by him.[14] For any value of γ, the relations of $0 < a(\gamma) < 1$, $0 < \Delta(\gamma) < 1$ are to be satisfied. Although the plot of $\log(\chi_P T)$ *vs.* $1/T$ (not shown) gives rise to a linear relation between them, the regression yields contradictory values of $a(\gamma)$ and $J_1\Delta(\gamma)$ as follows

$$a(\gamma) = 3.8, \quad J_1\Delta(\gamma) = 0.15\,\text{eV}.$$

This contradiction could originate in the temperature dependence of the alternation parameters, J_1 and/or γ. When both J_1 and γ are temperature dependent, each of J_1 and γ cannot be determined uniquely from our susceptibility measurements, but the possible combinations of (J_1, γ) can be determined so as to reproduce the observed value of χ_P at T by using Eq. 5. In Fig. 8, the determined combinations are plotted as a function of temperature over the range of J_1 from 0.10 to 0.16 eV. A curved plane is obtained for the possible set of parameters (J_1, γ, T). When J_1 is assumed to be constant, γ increases with increasing temperature. Such behavior of γ means that the spin system varies from the singlet-triplet model to Heisenberg one with increasing temperature. When γ is assumed to be constant contrariwise, J_1 decreases with increasing temperature. Thus, the

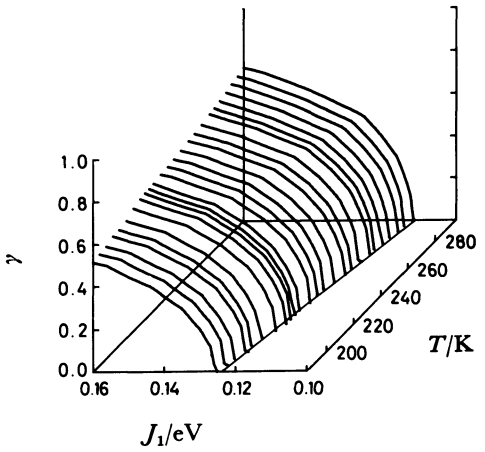

Fig. 8. Temperature variation of possible combination of (J_1, γ). The curves are not smooth, because the numerical values of $a(\gamma)$ and $\Delta(\gamma)$ in Eq. 5 are given for the values of γ in every 0.1 step.[14]

curved plane in Fig. 8. seems to be reasonable phenomenologically. In other words, the observed temperature dependence of χ_P could be explained by the linear alternating antiferromagnetic Heisenberg model with the rational temperature dependence of the alternation parameters. We expect the value of γ to be somewhat large (*e.g.*, 0.3—0.5) in NMPN on the basis of the absence of the fine structure and the transitions of $\Delta m=\pm 2$ in the ESR measurements.

Such temperature dependence of the alternation parameters resembles the prediction made by the theoretical studies of the spin-Peierls transition. It is known from these studies that the presence of the spin-lattice[24,27,28] or spin-phonon[22,27,28] interactions in an uniform chain system results in a phase transition to an alternating chain, indicating temperature dependence of alternation parameters. This predicted temperature dependence is similar to that observed in our material. The decompositions of the radical molecules above room temperature prevent us from getting the information about the phase transition and therefore we cannot apply the theory of the spin-Peierls transition to our problem at present. However, we preferably think that the spin-lattice or spin-phonon interaction plays an important role in the magnetic behavior of our material.

Comparison of NMPN and NEP

The comparison of properties of organic solids whose components have similar molecular structure is important in chemistry, especially for molecular designing. 10-Ethyl-5-phenazinyl (NEP) is a member of the phenazinyl family and has well been studied. Therefore NMPN and NEP are compared with each other below.

NEP was investigated by Hausser[31] and Hausser and Murrell[32] first. They discovered the charge transfer absorption in the near IR region. Sakata and Nagakura[33] measured the temperature dependence of the CT-band intensity and of the magnetic properties in detail. They found that the properties of NEP were explained as the isolated spin pairs almost quantitatively. The existence of the charge transfer interactions is thus common to the two radicals. In ESR studies of NEP, however, the fine structure and the transitions of $\Delta m=\pm 2$ are found[33] and therefore its magnetic excited state is described by the spin Hamiltonian (3). The comparison of the two radicals is summarized in Table 2.

Table 2. The comparison of NMPN and NEP

	NMPN	NEP[a]
$h\nu_{CT}$/eV	1.08	1.38
J/eV	0.11[b]	0.04
Fine structure and transition of $\Delta m=\pm 2$	not observed	observed

a) in Ref. 33. b) The magnetic excitation gap at room temperature calculated from Eq. 2.

The most remarkable difference is the magnitude of the interpair interactions. The ESR behaviour of NEP is described by the spin Hamiltonian of noninteracting pair, whereas that of NMPN is not. This difference would arise from the steric factor. The steric hindrance due to the ethyl group in NEP seems to be so large that the interpair interactions are prevented. This difference has something in common with that of the crystal structures of *N*-methylphenazinium(NMP)-TCNQ and other *N*-alkylphenazinium-TCNQ complexes. NMP-TCNQ is a famous organic conductor and forms segregated columns in the crystal. NMP molecules in the columns stack uniformly.[34] On the other hand, NEP_2-$TCNQ_2$ crystallizes in mixed stacks with σ-bonded dimers of $(TCNQ)_2^{2-}$.[35] *N*-butylphenazinium (NBP)-TCNQ[36] and NBP-F_4TCNQ[37] comprise -AADD- type mixed stacks. Replacement of the methyl group of NMP by a larger alkyl group therefore seems to hinder the interactions beyond the intradimer ones.

The maximum position of the CT-band of NMPN is lower than that of NEP by about 0.30 eV. In terms of the Hubbard model,[38] it is known that when the on-site Coulomb repulsion U is much larger than the transfer integral t the position of the CT-band maximum is almot determined only by U.[39] Therefore, the relation of the on-site Coulomb repulsion of the two radicals is established as;

$$U_{NMPN} < U_{NEP}.$$

It is likely that the nitrile group in NMPN extends the conjugation system of the phenazinyl frame and the extention decreases the on-site repulsion.

The magnetic excitation gap J of NMPN is about three times as large as that of NEP at room temperature. This gap is approximated by the equation $J=(1/2)(U^2+16\,t^2)^{1/2}-U/2$. The difference of U is not so large that the following relation of the intrapair hopping integrals would be established;

$$t_{NMPN} > t_{NEP}.$$

The Electric Conductivity of Neutral Radicals

Finally, we discuss the way to obtain more conductive neutral radicals by referring to the electric conductivity of NMPN. As described in a previous section, NMPN is much more conductive than the other neutral radicals which are thought to be stabilized by the protective subtituents and is placed in the most conductive class of organic solids

composed of one kind of molecules. In comparison with recent "organic metals", however, the conductivity of NMPN is still much poor.

The factors which raise the conductivity of NMPN are summarized as follows.

1) The existence of the unpaired electron on the each molecule.

2) The planar molecular structure giving the expectancy of large molecular overlaps.

3) The small substituent.

It is clear from our studies that the second and the third factors are necessary conditions to give neutral radicals higher conductivity. These factors mean that the neutral radical should be stabilized not by the protective substituents, but by the intramolecular delocalization energy of unpaired electron.

On the other hand, the conductivity of NMPN would be suppressed by the following factors.

1) The nonuniform interactions between unpaired electrons which are localized, to some extent, within a pair.

2) The electron localization due to the fully-occupied Hubbard band with large U (Mott insulator).

In order to produce new neutral radicals having higher conductivity than that of NMPN, these factors should be improved. One of the possibilities for improvement is to find neutral radicals containing heavy atoms that are expected to have interactions comparable with or beyond the intrapair ones. In this case, we could further expect the effect of interchain interaction, if the heavy atoms are properly chosen. The problem of electron localization would also be relaxed, to some extent, by introducing heavy atoms with large polarizability and large van der Waals radius, because such heavy atoms would reduce the magnitude of U and increase the transfer integral. Another way to reduce the electron localization is to make a mixed crystal of a neutral radical and a closed shell compound, which has molecular structure similar to the radical molecule and has HOMO or LUMO of energy nearly equivalent to the nonbonding molecular orbital of the neutral radical. In such a crystal, if exist, it would be possible that the nonbonding MO of the neutral radicals and HOMO or LUMO of the closed shell molecules make the band partially filled, in which electrons or holes are delocalized. In the case of NMPN, the mixed crystal of NMPN and phenazine or 5,10-dialkyl-5,10-dihydrophenazine could be a possible candidate.

The authors are thankful to Professor Kazuo Morigaki and Dr. Izumi Hirabayashi of Institute for Solid State Physics for the kindness in putting the ESR spectrometer at their disposal. This work was in part supported by the Grant-in-Aid for Scientific Research (Nos. 58118003, 58470003, and 59112003) from the Ministry of Education, Science and Culture.

References

1) For a review see F. Gutmann and L. E. Lyons, "Organic Semiconductor," J. Wiley, New York (1967).

2) D. D. Eley and H. Inokuchi, *Z. Electrochem.*, **63**, 29 (1959).

3) D. D. Eley and M. R. Willis, "Symposium on Electrical Conductivity in Organic Solids," ed by H. Kallmann and M. Silver, Interscience Pub., London (1961), p. 257.

4) H. Inokuchi, Y. Harada, and Y. Maruyama, *Bull. Chem. Soc. Jpn.*, **35**, 1559 (1962).

5) D. E. Williams, *J. Am. Chem. Soc.*, **89**, 4280 (1967).

6) D. E. Williams, *Mol. Phys.*, **16**, 145 (1969).

7) H. McIlwain, *J. Chem. Soc.*, **1937**, 1704.

8) M .Takahashi, T. Sugano, and M. Kinoshita, *Bull. Chem. Soc. Jpn.*, **57**, 26 (1984).

9) We employed in this report the c.g.s. electromagnetic units for magnetic susceptibility, in the interest of comparison with values in references. The χ values given in emu mol^{-1} are converted into the SI units of $m^3\ mol^{-1}$ by multiplying the factor of $4\pi\times10^{-6}$.

10) Y. Sato, M. Kinoshita, M. Sano, and H. Akamatu, *Bull. Chem. Soc. Jpn.*, **43**, 2370 (1970).

11) H. M. McConnell and Z. G. Soos, *J. Chem. Phys.*, **40**, 586 (1964).

12) D. B. Chesnut, *J. Chem. Phys.*, **41**, 472 (1964).

13) L. N. Bulaevskii, *Zh. Eksp. Teor. Fiz.*, **44**, 1008 (1963) (*Sov. Phys. **JETP**,* **17**, 684 (1963)).

14) L. N. Bulaevskii, *Fiz. Tverd. Tela (Leningrad),* **11**, 1132 (1969) (*Sov. Phys. Solid State,* **11**, 921 (1969)).

15) Z. G. Soos, *J. Chem. Phys.*, **43**, 1121 (1965); *ibid.*, **46**, 253 (1967).

16) W. Duffy, Jr. and K. P. Barr, *Phys. Rev.*, **165**, 647 (1968).

17) J. C. Bonner, H. W. J. Blöte, J. W. Brag, and I. S. Jacobs, *J. Appl. Phys.*, **50**, 1810 (1979).

18) N. Mataga and T. Kubota, "Molecular Interactions and Electronic Spectra," Marcel Dekker, Inc., New York (1970), P. 275.

19) S. K. Lyo, *Phys. Rev. B,* **18**, 854 (1978).

20) S. K. Lyo, *Phys. Rev. B,* **18**, 5835 (1978).

21) T. Yamazaki and K. Kimura, *Bull. Chem. Soc. Jpn.*, **44**, 298 (1971).

22) E. Pytte, *Phys. Rev. B,* **10**, 4637 (1974).

23) S. Etemad and E. Ehrenfreund, *AIP Conf. Proc.*, **10**, 1499 (1973); S. K. Khanna, E. Ehrenfreund, E. F. Rybaczewski, and S. Etemad, *AIP Conf. Proc.*, **10**, 1509 (1973).

24) G. Beni, *J. Chem. Phys.*, **58**, 3200 (1973).

25) T. Todani and K. Kawasaki, *Prog. Theor. Phys.*, **50**, 1216 (1973).

26) L. N. Bulaevskii, *Zh. Eksp. Teor. Fiz.*, **43**, 968 (1962) (*Sov. Phys. **JETP**,* **16**, 685 (1963)).

27) P. Pincus, *Solid State Commun.*, **9**, 1971 (1971).

28) G. Beni and P. Pincus, *J. Chem. Phys.*, **57**, 3531 (1972).

29) J. Y. Dubois and J. B. Carton, *J. Phys. (Paris),* **35**, 371 (1974).

30) E. Pytte, *Phys. Rev. B,* **10**, 2039 (1974).

31) K. H. Hausser, *Z. Naturforsh., Teil A,* **11**, 20 (1956).

32) K. H. Hausser and J. N. Murrell, *J. Chem. Phys.*, **27**, 500 (1957).
33) T. Sakata and S. Nagakura, *Bull. Chem. Soc. Jpn.*, **42**, 1497 (1969).
34) C. J. Fritchie Jr., *Acta Crystallogr.*, **20**, 892 (1966); B. Morosin, *Phys. Lett. A*, **53**, 455 (1975).
35) B. Morosin, H. J. Plastas, L. B. Coleman, and J. M. Stewart, *Acta Crystallogr., Sect. B*, **34**, 540 (1978).
36) D. Gundel, H. Sixl, R. M. Metzger, N. E. Heimer, R. H. Harms, H. J. Keller, D. Nöthe, and D. Wehe, *J. Chem. Phys.*, **79**, 3678 (1983).
37) R. M. Metzger, N. E. Heimer, D. Gundel, H. Sixl, R. H. Harms, H. J. Keller, D. Nöthe, and D. Wehe, *J. Chem. Phys.*, **77**, 6023 (1982).
38) J. Hubbard, *Proc. R. Soc. London, Ser. A*, **276**, 278 (1963); *ibid.*, **281**, 401 (1964).
39) I. Sadakata and E. Hanamura, *J. Phys. Soc. Jpn.*, **34**, 882 (1973).